Identification of SARS-CoV-2 3CL Protease Inhibitors by a Quantitative High-throughput Screening

Wei Zhu[#], Miao Xu[#], Catherine Z. Chen, Hui Guo, Min Shen, Xin Hu, Paul Shinn, Carleen Klumpp-Thomas, Samuel G. Michael, Wei Zheng[*]

National Center for Advancing Translational Sciences, National Institutes of Health, Rockville, MD 20850, USA

[#]These authors contributed equally to this work

*To whom correspondence should be addressed:

Wei Zheng, Ph.D., wzheng@mail.nih.gov

Running title: SARS-CoV-2 3CL protease screening

Word count: 3661

Abbreviations: SARS-CoV-2, severe acute respiratory syndrome coronavirus 2; COVID-19, coronavirus disease 2019; $3CL^{pro}$, 3C like protease; qHTS, quantitative high throughput screening.

Key words: SARS-CoV-2, COVID-19, main protease, 3CL protease, enzyme inhibitor

Bullet point summary:

What is already known

- SARS-CoV-2 $3CL^{pro}$ is a valid target for drug development.

What this study adds

- Identification of 27 inhibitors of SARS-CoV-2 $3CL^{pro}$ by a qHTS of 10,755 compounds consisting of approved and investigational drugs, and bioactive compounds.

Clinical significance

- Some of the newly identified $3CL^{pro}$ inhibitors can be evaluated in drug combination therapy for synergistic effect to treat COVID-19 patients, while the others can serve as starting points for medicinal chemistry optimization to improve potency and drug like properties for drug development.

Background and Purpose:

The COVID-19 caused by SARS-CoV-2 has emphasized the urgent need for therapeutic development. Drug repurposing screening is the most practical and rapid approach for discovery of such therapeutics. The $3CL^{pro}$, or main protease (M^{pro}) of SARS-CoV-2 is a valid drug target as it is a viral enzyme with an essential role in viral replication, and cleavage specificity that is distinct from host proteases.

Experimental Approach:

We employed and miniaturized a fluorogenic $3CL^{pro}$ enzyme assay in which $3CL^{pro}$ cleaves a quenched peptide substrate and releases a fluorescent fragment, resulting an increase in fluorescence signal. By using this SARS-CoV-2 $3CL^{pro}$ assay, we conducted a qHTS of 10,755 compounds consisting of approved and investigational drugs, and bioactive compounds, at 4 compound concentrations. The confirmed $3CL^{pro}$ inhibitors were also tested in a SARS-CoV-2 cytopathic effect assay to determine their effects on rescuing of cell death caused by the virus infection.

Key Results:

Twenty-seven small molecule inhibitors of SARS-CoV-2 $3CL^{pro}$ have been identified with IC_{50}s ranging from 0.26 to 27.1 μM with a greater than 80% maximal inhibition. Walrycin B (IC_{50} = 0.26 μM), Hydroxocobalamin (IC_{50} = 3.29 μM), Suramin sodium (IC_{50} = 6.50 μM), Z-DEVD-FMK (IC_{50} = 6.81 μM), and LLL-12 (IC_{50} = 9.84 μM) are the most potent $3CL^{pro}$ inhibitors with IC_{50}s under 10 μM. The activities of anti-SARS-CoV-2 viral infection were confirmed in 11 of 27 compounds.

Conclusion and Implications:

Some of the newly identified inhibitors of SARS-CoV-2 $3CL^{pro}$ may be used in combination therapy with other drugs for synergistic effect to treat COVID-19 patients. The other inhibitors found in this study can provide starting points for medicinal chemistry optimizations.

Introduction

Coronavirus disease 2019 (COVID-19) has rapidly become a global pandemic since the first case was found in late 2019 in China. The causative virus was shortly confirmed as severe acute respiratory syndrome coronavirus 2 (SARS-CoV-2), which is a positive-sense single RNA virus consisting of four structural proteins and an RNA genome. Upon entering the host cell, the viral genome is translated to yield two overlapping polyproteins-pp1a and pp1ab (Jin et al., 2020; Wu et al., 2020). 3CL protease ($3CL^{pro}$, also called main protease) of the related virus is excised from the polyproteins by its own proteolytic activity (Thiel et al., 2003), and subsequently work together with papain-like protease to cleave the polyproteins to generate total 16 functional non-structural proteins (nsps). It was reported that the $3CL^{pro}$ of SARS specifically operates at 11 cleavage sites on the large polyprotein 1ab (790 kDa) (Thiel et al., 2003), and no human protease has been found to share similar cleavage specificity (Zhang et al., 2020). The cleaved nsps play essential roles in assembling the viral replication transcription complex (RTC) to initiate the viral replication. Although vaccine development is critically important for COVID-19, effective small molecule antiviral drugs are urgently needed. Because of its essential role and no human homolog, $3CL^{pro}$ is one of the most intriguing drug targets for antiviral drug development (Anand, Ziebuhr J Fau - Wadhwani, Wadhwani P Fau - Mesters, Mesters Jr Fau - Hilgenfeld & Hilgenfeld, 2003; Zhang et al., 2020). The inhibitors of $3CL^{pro}$ are most likely less-toxic to host cells (Zhang et al., 2020).

Viral protease has been investigated as a drug target for decades resulting in several approved drugs for human immunodeficiency viruses (HIV) and hepatitis C virus (HCV) (De Clercq & Li, 2016). Saquinavir was the first approved protease inhibitor for HIV, which started an era for this new class of antiviral drugs with the approval in 1995 (De Clercq & Li, 2016). Saquinavir contains a hydroxyethylene bond, which functions as a peptidomimetic scaffold to block the catalytic function of the protease. Some of other approved protease inhibitors for HIV, such as ritonavir, nelfinavir, indinavir, lopinavir, amprenavir, atazanavir, fosamprenavir, and darunavir, share the similar inhibition mechanism with saquinavir (De

Clercq & Li, 2016). In addition to HIV, another group of approved viral protease inhibitors is used for treatment of HCV. Although the structure of HCV is different compared to HIV, the same function in cleaving viral precursor proteins renders the HCV protease a valid target for antiviral drug development. Asunaprevir, boceprevir, simeprevir, paritaprevir, vaniprevir, telaprevir, and grazoprevir, etc. have been approved by FDA for treatment of HCV (De Clercq & Li, 2016). Regarding the coronavirus, the effort to target the SARS-CoV and SARS-CoV-2 $3CL^{pro}$ has identified several drug candidates (Blanchard et al., 2004). However, to date, no $3CL^{pro}$ inhibitor has been specifically approved for SARS-CoV or SARS-CoV-2.

In this study, we have employed a SARS-CoV-2 $3CL^{pro}$ assay that uses a self-quenched fluorogenic peptide substrate for a quantitative high throughput screen (qHTS) (Inglese et al., 2006) of 10,755 compounds including approved drugs, clinically investigated drug candidates, and bioactive compounds. We report here the identification of 27 $3CL^{pro}$ inhibitors with the IC_{50} ranging from 0.3 to 30 μM and maximal inhibition over 80%. The results from this study can contribute to the design of the synergistic drug combinations for treatment of COVID-19 as well as new starting points for lead optimization of SARS-CoV-2 $3CL^{pro}$ inhibitors.

Materials and Methods

Materials

$3CL^{pro}$ of SARS-CoV-2 with an N-terminal MBP-tag, sensitive internally quenched fluorogenic substrate, and assay buffer were obtained from BPS Bioscience (San Diego, CA, USA). The enzyme was expressed in E. coli expression system, has a molecular weight of 77.5 kDa. The peptide substrate contains 14 amino sequence (KTSAVLQSGFRKME) with Dabcyl and Edans attached on its N- and C-terminals, respectively. The reaction buffer is composed of 20 mM Tris-HCl (pH 7.3), 100 mM NaCl, 1 mM EDTA, 0.01 % BSA (bovine serum albumin), and 1 mM 1,4-dithio-D, L-threitol (DTT). GC376 (CAS No: 1416992-39-6) was purchased from Aobious (Gloucester, MA, USA). Library of Pharmacologically Active Compounds

(LOPAC) was purchased from Sigma-Aldrich (St. Louis, MO, USA). All other compound libraries were sourced by the National Center for Advancing Translational Sciences (NCATS) including the NCATS Pharmaceutical Collection (NPC) (Huang et al., 2019), anti-infective, MIPE5.0, and NPACT libraries. LOPAC library has 1280 compounds consisting of marketed drugs and pharmaceutically relevant structures with biological activities. NPC library contains 2552 FDA approved drugs, investigational drugs, animal drugs and anti-infectives. Anti-infective library is a NCATS collection that contains 739 compounds that specifically target to viruses. MIPE 5.0 library includes 2480 compounds that are mixed with approved and investigational compounds, and mechanistic based compounds focusing on oncology. NPACT library contains 5099 structurally diverse compounds consisting of approved drugs, investigational drugs, and natural products.

3CL^{pro} enzyme assay

The 3CL^{pro} enzyme assay was developed in 384-well black, medium binding microplates (Greiner Bio-One, Monroe, NC, USA) with a total volume of 20 µL and then miniaturized to 1536-well format. In 384-well plate format, 10 µL enzyme in reaction buffer was added into each well, followed by the addition of 10 µL substrate. Fluorescent intensity was measured at different time points on a PHERAstar FSX plate reader (BMG Labtech, Cary, NC, USA) with Ex=340 nm/Em=460 nm after the addition of substrate. The experiment was conducted at both room temperature (RT) and 37 °C.

Steady-state kinetic parameters were evaluated using 50 nM 3CL^{pro} and different concentrations of substrate. In brief, 10 µL/well enzyme was added into 384-well plate. The reaction was then initialized by adding the substrate solutions at different concentrations. The substrate stock solution was serially diluted 1:2 to obtain seven concentrations. The final concentrations used in this test were 160, 80, 40, 20, 10, 5, and 2.5 µM. The fluorescent intensity was measured at 5, 10, 15, and 30 min.

Compound library screening, confirmation and counter screen

For the primary screen, library compounds were formatted in 1536-well plates with 4 compounds concentrations at inter-plate titration of 1:5 with the highest concentration of 10 mM for most of compounds in the libraries. The SARS-CoV-2 $3CL^{pro}$ assay was initiated by dispensing 2 μL/well of 50 nM enzyme solution into 1536 black bottom microplates (Greiner Bio-One, Monroe, NC, USA) by a Multidrop Combi disperser (Thermo Fisher Scientific, Waltham, MA, USA), followed by pin transfer of 23 nL compounds in DMSO solution using an automated pintool workstation (WAKO Scientific Solutions, San Diego, CA). After 30 min incubation at RT, 2 μL/well 20 μM substrate solution was dispensed into the assay plates to initiate the enzyme reaction. After 3 h incubation at RT, the plates were read at 460 nm emission upon excitation at 340 nm.

Following primary screening, selected hit compounds were diluted with intraplate 11-point dilution at 1:3 ratio and tested using the same enzyme assay as the primary screen. Each compound was tested in three biological replicates.

A counter-screen assay to eliminate the fluorescence quenching compounds was carried out by dispensing 4 μL of 0.8 μM fluorescent Edans fragment, SGFRKME-Edans, into 1536-well assay plates. Compounds were pin transferred as 23 nL/well and the fluorescence signal was read.

SARS-CoV-2 cytopathic effect (CPE) assay

SARS-CoV-2 CPE assay was conducted at Southern Research Institute (Birmingham, AL) as described in previous reports (Chen et al., 2020; Gorshkov et al., 2020). In brief, high ACE2 expressing Vero E6 cells were inoculated with SARS-CoV-2 (USA_WA1/2020) at 0.002 M.O.I. After infection of 72 h at 37 °C and 5% CO_2, the cell viability was examined with CellTiter-Glo ATP content assay kit (Promega, Madison, WI, USA). CPE raw data were normalized to non-infected cells and virus infected cells only which were set as 100% efficacy and 0 efficacy, respectively. In addition, the compound cytotoxicity was evaluated in the same cells by measuring ATP content in the absence of virus. Compound cytotoxicity raw data were

normalized with wells containing cells only as 100 % viability (0% cytotoxicity), and wells containing media only as 0% viability (100% cytotoxicity).

Modeling

Modeling and docking studies were performed using the Molecular Operating Environment (MOE) program (Chemical Computing Group ULC, Montreal, QC, Canada). The crystal structure of $3CL^{pro}$ in complex with a peptide-like inhibitor N3 (PDB code 6LU7) (Jin et al., 2020) was used to dock inhibitors to the active site of $3CL^{pro}$. The ligand induced fit docking protocol was used and the binding affinity was evaluated using the GBVI/WSA score. Covalent docking was performed for inhibitors Z-DEVD-FMK and Z-FA-FMK, with a covalent binding to residue Cyc145. Finally, energy minimization was performed to refine the predicted binding complex.

Data analysis and statistics

The primary screen data was analyzed using a customized software developed in house at NCATS (Huang et al., 2019). Raw data were normalized to relative controls, in which the DMSO alone was set as 0% inhibitory activity, the reaction buffer containing substrate only was set as 100% inhibitory activity. Concentration-response curves were fitted and IC_{50} values of confirmed compounds were calculated using the GraphPad Prism software (San Diego, CA, USA). Data are presented as mean ± standard deviation (SD). Statistical significance was analyzed using one-way ANOVA and difference was defined as $P<0.05$.

Results

Optimization of enzyme and substrate concentrations for $3CL^{pro}$ enzyme assay

To carry out a qHTS of SARS-CoV-2 $3CL^{pro}$ inhibitors, a fluorogenic protease enzyme assay was used and optimized. As illustrated in **Figure 1,** the C-terminal of a peptide substrate links to a fluorophore (Edans) and the N-terminal has a fluorescence quencher (Dabcyl) that quenches the fluorescence signal of Edans.

When the $3CL^{pro}$ hydrolyzes the substrate to yield two fragments, Dabcyl is separated with Edans, which relieves the fluorescence quenching effect resulting in an increase of fluorescence signal.

To optimize the assay conditions, different enzyme concentrations were first examined in this enzyme assay at 20 μM substrate concentration in a 384-well plate (**Figure 2a**). The signal-to-basal (S/B) ratio increased with the incubation times for all 3 enzyme concentrations tested (**Figure 2b**). The 120 min incubation resulted in S/B ratios of 2.4, 3.8, and 6.0-fold for enzyme concentrations of 25, 50 and 100 nM, respectively. We selected 50 nM enzyme concentration as an optimized condition for subsequent experiments.

Enzyme kinetic study was then conducted to determine the Km and Vmax of this viral protease. Substrate concentrations ranging from 2.5 to 160 μM were used in this experiment with a fixed 50 nM enzyme (**Figure 2c**). The Km was 75.41 μM and the Vmax was 1392 RFU/min for this recombinant SARS-CoV-2 $3CL^{pro}$. For a consideration of assay sensitivity, it is desirable to use the lowest enzyme concentration and substrate concentration (ideally under Km value) that still yield reliable S/B ratio (assay window, usually > 2-fold). Because inhibitors usually compete with substrates for binding to the free enzyme, a high substrate concentration can reduce potencies (IC_{50}s) of inhibitors determined in enzyme assays (Copeland, 2003). Thus, 50 nM $3CL^{pro}$ and 20 μM substrate were selected as the optimized conditions for qHTS. We also found that the assay performance at 37 °C was similar to that at RT. Therefore, the subsequent compound screens were conducted at RT (**Figure 2d**).

Validation of $3CL^{pro}$ enzyme assay with a known protease inhibitor and measurements of HTS assay parameters

To validate the enzyme assay, a known SARS-CoV-2 $3CL^{pro}$ inhibitor, GC376 (Ma et al., 2020), was evaluated in 1536-well plate format. GC376 concentration-dependently inhibited the enzyme activity of SARS-CoV-2 $3CL^{pro}$ with an IC_{50} value of 0.17 μM. The highest tested concentration of GC376 (57.5 μM) exhibited a complete inhibition, where the fluorescent intensity was equal to the background substrate in

the absence of enzyme. This IC_{50} value of GC376 is comparable to the reported value (Ma et al., 2020), indicating the reliability of this enzymatic assay (**Figure 3a**).

Since DMSO is the solvent for all compounds in our compound libraries, we tested a DMSO plate in 1536-well plate for the assessment of HTS assay parameters. A S/B ratio of 3.47-fold, a coefficient of variation (CV) of 4.9% and a Z' factor of 0.71 were obtained in the 1536-well DMSO plate test, indicating this enzyme assay is robust for HTS (**Figure 3b**).

Drug repurposing screen for 3CL^{pro} enzyme inhibitors

A primary screen of 10,755 compounds in the libraries containing approved drugs, investigational drug candidates, and bioactive compounds yielded 161 hits in which the hit rate was 1.5 % (Figure S1). Since the primary screen was done in four compound concentrations, compounds in dose-response curve classes 1-3 were selected as hits from the primary screen (Inglese et al., 2006; Wang, Jadhav, Southal, Huang & Nguyen, 2010). These primary hits were then "cherry-picked" for confirmation test in the same enzyme assay. Hit confirmation was performed at 11 compound concentrations at 1:3 titration. The confirmed hits were selected using a cutoff of maximal inhibition greater than 80 % and IC_{50} less than 30 μM. The results of primary screening and hit confirmation have been uploaded into the NCATS Open Data Portal for public access (Brimacombe et al., 2020).

Because this SARS-CoV-2 3CL^{pro} assay is a fluorogenic assay, compounds with fluorescence quenching properties can suppress the fluorescence signal generated by the protease activity. To eliminate the false positives, we conducted a counter screen to identify compounds that quench the fluorescence of SGFRKME-Edans, the product of the 3CL^{pro} enzyme reaction, in the absence of the protease enzyme. Based on the standard curve (Figure S2), the 3CL^{pro} assay conditions generated signals that matched 0.8 μM of Edans fragment. Results indicated that no compound with over 80% inhibition to 3CL^{pro} activity showed fluorescence quenching effect. In summary, 27 compounds were confirmed that inhibited SARS-CoV-2 3CL^{pro} activity with IC_{50} values < 30 μM and maximal inhibition > 80% (**Table 1**). Five of these compounds

have IC_{50} less than 10 μM that are the most potent among these 27 confirmed compounds (**Figure 4)**. In addition, 21 compounds have maximal inhibition between 50% to 80%. Five of them showed remarkable quenching effect and have been eliminated which resulted in 16 compounds with inhibitory activity against the $3CL^{pro}$ (Table S1).

Confirmation of antiviral activity of $3CL^{pro}$ inhibitors in a SARS-CoV-2 live virus assay

To evaluate the antiviral effect of these $3CL^{pro}$ inhibitors against infections of SARS-CoV-2 virus, we tested the confirmed inhibitors in a CPE assay. Amongst them, Z-FA-FMK, anacardic acid, and MG-149 showed the highest rescue of SARS-CoV-2 induced CPE with the efficacies of 104.85%, 89.63%, and 70%, respectively. The protease inhibitor Z-FA-FMK inhibited viral CPE with an EC_{50} of 0.13 μM, with no apparent cytotoxicity. For the five most potent compounds in the $3CL^{pro}$ enzyme assay, hydroxocobalamin and Z-DEVP-FMK were neither effective in CPE assay, nor cytotoxic to Vero E6 cells. Walrycin B and LLL-2 showed apparent toxicity with CC50 values of 10 μM and 1.77 μM, and full cytotoxicity levels. There was poor correlation between the $3CL^{pro}$ enzyme and CPE assays. This could be due to cytotoxicity of compounds obscuring CPE effects in live cells. Also, polypharmacology could contribute, as compounds with higher potency in the CPE assay compared to the $3CL^{pro}$ enzyme assay might also have other target(s). In addition, the CPE assay may be less sensitive to certain drugs in this CPE because the cell death caused by SARS-CoV-2 infection in Vero 6 cells is a special *in vitro* assay condition that may not fully represent the virus infection in human.

Modeling analysis

We docked the identified compounds to the active site of $3CL^{pro}$ to further investigate their potential binding to the protease target. The peptide-like inhibitors Z-DEVD-FMK and Z-FA-FMK fit well in the active site of $3CL^{pro}$ by forming a covalent bond between the keto and the catalytic residue Cys145, while the side groups were orientated to the S1, S2 and S4 pocket (**Figure 5**). Small molecule inhibitors like Walrycin B and LLL-12 were found to bind to the S1 or S1' pocket near Cys145, but no specific binding interactions

were observed. Most of other compounds such as Suramin sodium and Hydroxocobalamin did not dock in the active site of $3CL^{pro}$ and appeared not to be protease inhibitors.

Discussion

Viral protease is a valid antiviral drug target for RNA viruses including coronaviruses (Zumla, Chan, Azhar, Hui & Yuen, 2016). In response to the COVID-19 pandemic, great efforts have been made to evaluate the possibility of repurposing approved viral protease inhibitor drugs for the clinical treatment of the disease. Unfortunately, the combination of lopinavir and ritonavir, both approved HIV protease inhibitors, failed in a clinical trial without showing benefit compared to the standard of care (Cao et al., 2020). To address this unmet need, several virtual screens and a drug repurposing screen were performed to identify SARS-CoV-2 $3CL^{pro}$ inhibitors. Ma et al. screened a focused collections of protease inhibitors using an enzyme assay and identified Boceprevir, GC376, and three calpain/cathepsin inhibitors as potent SARS-CoV-2 $3CL^{pro}$ inhibitors (Ma et al., 2020). Amongst them, Boceprevir, an FDA-approved HCV drug, not only showed the inhibition of $3CL^{pro}$ with an IC_{50} of 4.13 μM, but also has an EC_{50} of 1.90 μM against SARS-CoV-2 virus infection in the CPE assay (Ma et al., 2020). Lopinavir and ritonavir did not show inhibition to $3CL^{pro}$ in the study that indicated both of them have weak inhibitory activity against SARS-CoV-2 $3CL^{pro}$.

In the virtual screen efforts, novel compounds were designed and synthesized by analyzing the substrate-binding pocket of SARS-CoV-2 $3CL^{pro}$. The two lead compounds, 11a and 11b, designed by Dai et al. presented high potency in both enzyme inhibition and anti-SARS-CoV-2 infection activity (Dai et al., 2020). In another more comprehensive study, Jin et al. identified six compounds that have IC_{50} values ranging from 0.67 to 21.4 μM against SARS-CoV-2 $3CL^{pro}$ by applying structure-assisted drug design and compound library repurposing screen (Jin et al., 2020).

In our qHTS of 10,755 compounds using the $3CL^{pro}$ enzyme assay, we identified 27 compounds that inhibited SARS-CoV-2 $3CL^{pro}$ enzymatic activity. Among 5 compounds with IC_{50} values under 10 μM,

walrycin B (IC_{50} = 0.27 μM) is the most potent inhibitor found in this screen. Walrycin B is an analog of toxoflavin (a phytotoxin from *Burkholderia glumae*) with potent activity of inhibiting bacteria growth. It was named as Walrycin B because it was found to inhibit the WalR activity in bacteria (Gotoh et al., 2010). The WalK/WalR two-component signal transduction system is essential for bacteria cell viability.

Hydroxocobalamin is a synthetic vitamin B12 (cobalamin) that is used in the clinics via intravenous administration. The antiviral effect of Vitamin B12 on HIV and HCV was reported previously. It was reported that Vitamin B12 inhibited the HIV integrase (Weinberg, Shugars, Sherman, Sauls & Fyfe, 1998). Li et al. reported that Vitamin B12 inhibited the HCV protein translation via the inhibition of HCV internal ribosome entry site (Li, Lott, Martyn, Haqshenas & Gowans, 2004). We found that hydroxocobalamin inhibited the SARS-CoV-2 $3CL^{pro}$ activity in this study.

Suramin is an FDA-approved anti-parasitic drug for trypanosomiasis and onchocerciasis and has to be given by intravenous injection as it has poor bioavailability when being taken orally (Barrett, Boykin, Brun & Tidwell, 2007). The IC_{50} for inhibition of SARS-CoV-2 $3CL^{pro}$ is 6.5 μM, which is much lower than the reported human plasma concentration of 97 - 181 μM (126 – 235 μg/ml) (Small et al., 2002). Suramin is an old drug with extensive polypharmacology (Wiedemar, Hauser & Mäser, 2020). Broad antiviral effects of suramin were reported including HIV, Dengue virus, Zika virus, Ebola virus, Hepatitis B and C viruses, Herpes simplex virus, Chikungunya virus, and Enterovirus (Wiedemar, Hauser & Mäser, 2020). The antiviral activity of suramin may be exerted through inhibiting viral entry and replication. Suramin can efficiently inhibit Chikungunya virus and Ebola envelope-mediated gene transfer to host cells (Henß et al., 2016). Multiple studies have also revealed that suramin interferes with viral RNA synthesis by targeting viral RNA-dependent RNA polymerase (Albulescu et al., 2015; Mastrangelo et al., 2012). A recent study by de Silva et al. demonstrated suramin inhibited SARS-CoV-2 replication in Vero E6 cells and reduced viral RNA in Calu-3 cells (da Silva et al., 2020). The authors proposed prevention of SARS-CoV-2 viral entry into cells as a mechanism of action. Different from these previously reported various mechanisms of

action, we found that suramin also targeted $3CL^{pro}$ enzyme of SARS-CoV-2, which is a new mechanism of action for this drug.

Another $3CL^{pro}$ inhibitor identified is Z-DEVD-FMK (IC_{50} = 6.81 μM). It is a cell permeable fluoromethyl ketone (FMK)-derivatized peptide acting as an irreversible caspase 3 inhibitor. It has been extensively studied as a neuroprotective agent as it inhibited caspase 3 induced apoptotic cell death in acute neurodegeneration (Barut et al., 2005; Knoblach, Alroy, Nikolaeva, Cernak, Stoica & Faden, 2004). Another similar peptide-like inhibitor Z-FA-FMK, a potent irreversible inhibitor of cysteine proteases including caspase 3, was also identified to inhibit $3CL^{pro}$ (IC_{50} = 12.1 μM). The predicted binding models of these inhibitors to $3CL^{pro}$ showed that they bound to the active site of $3CL^{pro}$ in the same manner as observed in other peptide-like $3CL^{pro}$ inhibitors (Jin et al., 2020), suggesting that they share the same mode of action for inhibition of $3CL^{pro}$ activity.

LLL-12 inhibited the $3CL^{pro}$ (IC_{50} = 9.84 μM) and it was originally generated by structure-based design targeting the signal transducer and activator of transcription 3 (STAT3) for cancer therapy, where it inhibited STAT3 phosphorylation and induced apoptosis (Lin et al., 2010). Antiviral activity of LLL-12 has been reported against HIV (Appelberg, Wallet, Taylor, Cash, Sleasman & Goodenow, 2017). The mechanism of action for its antiviral effect was unclear, though it suppressed HIV-1 infection in macrophages (Appelberg, Wallet, Taylor, Cash, Sleasman & Goodenow, 2017). In our current study, we found that LLL-12 inhibited the SARS-CoV-2 $3CL^{pro}$ activity.

In conclusion, this study employed an enzymatic assay for qHTS that identified 27 SARS-CoV-2 $3CL^{pro}$ inhibitors from a collection of approved drugs, drug candidates, and bioactive compounds. These $3CL^{pro}$ inhibitors can be combined with drugs of different targets to evaluate their potential in drug cocktails for the treatment of COVID-19. In addition, they can also serve as starting points for medicinal chemistry optimization to improve potency and drug like properties.

ACKNOWLEDGEMENTS

This work was supported by the Intramural Research Programs of the National Center for Advancing Translational Sciences, National Institutes of Health. The authors received no other financial supports for the research, authorship, and/or publication of this article.

CONFLICT OF INTEREST

The authors declare no conflicts of interest.

AUTHOR CONTRIBUTIONS

W.Zhu., M.X., X.H. performed the experiments. C.Z.C. and W.Zheng made the conceptualization. W.Zhu., H.G., M.S., X.H., W.Zheng. analyzed the data. W.Zhu., C.Z.C, W. Zheng., H.X., wrote the first draft of the manuscript. All others edited the manuscript.

References

Albulescu IC, van Hoolwerff M, Wolters LA, Bottaro E, Nastruzzi C, Yang SC, *et al.* (2015). Suramin inhibits chikungunya virus replication through multiple mechanisms. Antiviral Research 121**:** 39-46.

Anand K, Ziebuhr J Fau - Wadhwani P, Wadhwani P Fau - Mesters JR, Mesters Jr Fau - Hilgenfeld R, & Hilgenfeld R (2003). Coronavirus main proteinase (3CLpro) structure: basis for design of anti-SARS drugs. Science 300**:** 1763-1767.

Appelberg KS, Wallet MA, Taylor JP, Cash MN, Sleasman JW, & Goodenow MM (2017). HIV-1 Infection Primes Macrophages Through STAT Signaling to Promote Enhanced Inflammation and Viral Replication. AIDS Research and Human Retroviruses 33**:** 690-702.

Barrett MP, Boykin DW, Brun R, & Tidwell RR (2007). Human African trypanosomiasis: pharmacological re-engagement with a neglected disease. Br J Pharmacol 152**:** 1155-1171.

Barut Ş, Ünlü YA, Karaoğlan A, Tunçdemir M, Dağistanli FK, Öztürk M, *et al.* (2005). The neuroprotective effects of z-DEVD.fmk, a caspase-3 inhibitor, on traumatic spinal cord injury in rats. Surgical Neurology 64**:** 213-220.

Blanchard JE, Elowe NH, Huitema C, Fortin PD, Cechetto JD, Eltis LD, *et al.* (2004). High-throughput screening identifies inhibitors of the SARS coronavirus main proteinase. Chem Biol 11**:** 1445-1453.

Brimacombe KR, Zhao T, Eastman RT, Hu X, Wang K, Backus M, *et al.* (2020). An OpenData portal to share COVID-19 drug repurposing data in real time. bioRxiv**:** 2020.2006.2004.135046.

Cao B, Wang Y, Wen D, Liu W, Wang J, Fan G, *et al.* (2020). A Trial of Lopinavir-Ritonavir in Adults Hospitalized with Severe Covid-19. N Engl J Med 382**:** 1787-1799.

Chen CZ, Xu M, Pradhan M, Gorshkov K, Petersen J, Straus MR, *et al.* (2020). Identifying SARS-CoV-2 entry inhibitors through drug repurposing screens of SARS- S and MERS-S pseudotyped particles. bioRxiv**:** 2020.2007.2010.197988.

Copeland RA (2003). Mechanistic considerations in high-throughput screening. Anal Biochem 320**:** 1-12.

da Silva CSB, Thaler M, Tas A, Ogando NS, Bredenbeek PJ, Ninaber DK, *et al.* (2020). Suramin inhibits SARS-CoV-2 infection in cell culture by interfering with early steps of the replication cycle. Antimicrobial Agents and Chemotherapy**:** AAC.00900-00920.

Dai W, Zhang B, Jiang X-M, Su H, Li J, Zhao Y, *et al.* (2020). Structure-based design of antiviral drug candidates targeting the SARS-CoV-2 main protease. Science 368**:** 1331.

De Clercq E, & Li G (2016). Approved Antiviral Drugs over the Past 50 Years. Clin Microbiol Rev 29**:** 695-747.

Gorshkov K, Chen CZ, Bostwick R, Rasmussen L, Xu M, Pradhan M, *et al.* (2020). The SARS-CoV-2 cytopathic effect is blocked with autophagy modulators. bioRxiv**:** 2020.2005.2016.091520.

Gotoh Y, Doi A, Furuta E, Dubrac S, Ishizaki Y, Okada M, *et al.* (2010). Novel antibacterial compounds specifically targeting the essential WalR response regulator. The Journal of Antibiotics 63**:** 127-134.

Henß L, Beck S, Weidner T, Biedenkopf N, Sliva K, Weber C, *et al.* (2016). Suramin is a potent inhibitor of Chikungunya and Ebola virus cell entry. Virol J 13**:** 149-149.

Huang R, Zhu H, Shinn P, Ngan D, Ye L, Thakur A, *et al.* (2019). The NCATS Pharmaceutical Collection: a 10-year update. Drug Discovery Today 24**:** 2341-2349.

Inglese J, Auld DS, Jadhav A, Johnson RL, Simeonov A, Yasgar A, *et al.* (2006). Quantitative high-throughput screening: A titration-based approach that efficiently identifies biological activities in large chemical libraries. Proceedings of the National Academy of Sciences 103**:** 11473.

Jin Z, Du X, Xu Y, Deng Y, Liu M, Zhao Y, *et al.* (2020). Structure of Mpro from SARS-CoV-2 and discovery of its inhibitors. Nature 582**:** 289-293.

Knoblach SM, Alroy DA, Nikolaeva M, Cernak I, Stoica BA, & Faden AI (2004). Caspase Inhibitor z-DEVD-fmk Attenuates Calpain and Necrotic Cell Death in Vitro and after Traumatic Brain Injury. Journal of Cerebral Blood Flow & Metabolism 24**:** 1119-1132.

Li D, Lott WB, Martyn J, Haqshenas G, & Gowans EJ (2004). Differential Effects on the Hepatitis C Virus (HCV) Internal Ribosome Entry Site by Vitamin B₁₂ and the HCV Core Protein. Journal of Virology 78**:** 12075.

Lin L, Hutzen B, Li P-K, Ball S, Zuo M, DeAngelis S, *et al.* (2010). A novel small molecule, LLL12, inhibits STAT3 phosphorylation and activities and exhibits potent growth-suppressive activity in human cancer cells. Neoplasia 12**:** 39-50.

Ma C, Sacco MD, Hurst B, Townsend JA, Hu Y, Szeto T, *et al.* (2020). Boceprevir, GC-376, and calpain inhibitors II, XII inhibit SARS-CoV-2 viral replication by targeting the viral main protease. Cell Research.

Mastrangelo E, Pezzullo M, Tarantino D, Petazzi R, Germani F, Kramer D, *et al.* (2012). Structure-Based Inhibition of Norovirus RNA-Dependent RNA Polymerases. Journal of Molecular Biology 419**:** 198-210.

Small EJ, Halabi S, Ratain MJ, Rosner G, Stadler W, Palchak D, *et al.* (2002). Randomized Study of Three Different Doses of Suramin Administered With a Fixed Dosing Schedule in Patients With Advanced

Prostate Cancer: Results of Intergroup 0159, Cancer and Leukemia Group B 9480. Journal of Clinical Oncology 20**:** 3369-3375.

Thiel V, Ivanov KA, Putics Á, Hertzig T, Schelle B, Bayer S, *et al.* (2003). Mechanisms and enzymes involved in SARS coronavirus genome expression. Journal of General Virology 84**:** 2305-2315.

Wang Y, Jadhav A, Southal N, Huang R, & Nguyen D-T (2010). A grid algorithm for high throughput fitting of dose-response curve data. Curr Chem Genomics 4**:** 57-66.

Weinberg JB, Shugars DC, Sherman PA, Sauls DL, & Fyfe JA (1998). Cobalamin Inhibition of HIV-1 Integrase and Integration of HIV-1 DNA into Cellular DNA. Biochemical and Biophysical Research Communications 246**:** 393-397.

Wiedemar N, Hauser DA, & Mäser P (2020). 100 Years of Suramin. Antimicrobial Agents and Chemotherapy 64**:** e01168-01119.

Wu F, Zhao S, Yu B, Chen Y-M, Wang W, Song Z-G, *et al.* (2020). A new coronavirus associated with human respiratory disease in China. Nature 579**:** 265-269.

Zhang L, Lin D, Sun X, Curth U, Drosten C, Sauerhering L, *et al.* (2020). Crystal structure of SARS-CoV-2 main protease provides a basis for design of improved α-ketoamide inhibitors. Science 368**:** 409.

Zumla A, Chan JFW, Azhar EI, Hui DSC, & Yuen K-Y (2016). Coronaviruses - drug discovery and therapeutic options. Nature reviews Drug discovery 15**:** 327-347.

Table 1. Activity of 27 identified compounds against SARS-CoV-2 3CL^{pro}, and their CPE and cytotoxicity.

Compound Name	3CL^{pro} Inhibition		SARS-CoV-2 CPE		Vero E6 Cytotoxicity	
	IC_{50} (μM)	Max Resp (%)	EC_{50} (μM)	Efficacy (%)	CC_{50} (μM)	Efficacy (%)
Walrycin B	0.26	86.6	10	45.87	10	122.36
Hydroxocobalamin	3.29	89.56	N/A, >20	0	N/A, >20	0
Suramin sodium	6.5	99.49				
Z-DEVD-FMK	6.81	90.48	N/A, >20	0	N/A, >20	0
LLL-12	9.84	82.98	N/A, >20	0	1.77	100
Anacardic Acid	12.1	104.96	3.98	89.63	14.13	72.92
Z-FA-FMK	12.1	86	0.13	104.84	N/A, >20	0
NSC 95397	17.1	95.23				
(-)-Gossypol	19.18	115.46	N/A, >20	0	2.82	95.06
Adomeglivant	19.18	107.72	3.16	49.2	14.13	36.97
Tetradecylthioacetic acid	21.52	102.61				
Hexachlorophene	21.52	117.06	0.89	41.62	4.47	75.48
GW-0742	21.52	124.55	N/A, >20	0	N/A, >20	0
Sulfobromophthalein	21.52	103.89	N/A, >20	0	N/A, >20	0
GSK-3965	21.52	108.24	1.26	20.07	12.59	96.99
MK-886	21.52	109.11				
Agaric acid	21.52	106.38	N/A, >20	0	N/A, >20	0
Eltrombopag olamine	21.52	92.58	11.22	54.36	8.91	83.5
SU 16f	21.52	86.01	N/A, >20	0	7.94	23.57
Candesartan cilexetil (Atacand)	24.15	87.41	N/A, >20	0	12.59	80.08
Erythrosin B	24.15	120.23	N/A, >20	0	14.13	21.68
SH-4-54	24.15	98.36	N/A, >20	0	N/A, >20	0
Oritavancin (diphosphate)	24.15	93.29	N/A, >20	0	14.13	23.51
MX-69	24.15	92.69	7.94	13.22	N/A, >20	0
Penta-O-galloyl-β-D-glucose hydrate	27.1	106.92	7.08	39.5	12.59	34.55
MG-149	27.1	96.26	12.59	70	14.13	23.42
MK 0893	27.1	94.39	3.16	23.89	12.59	80.04

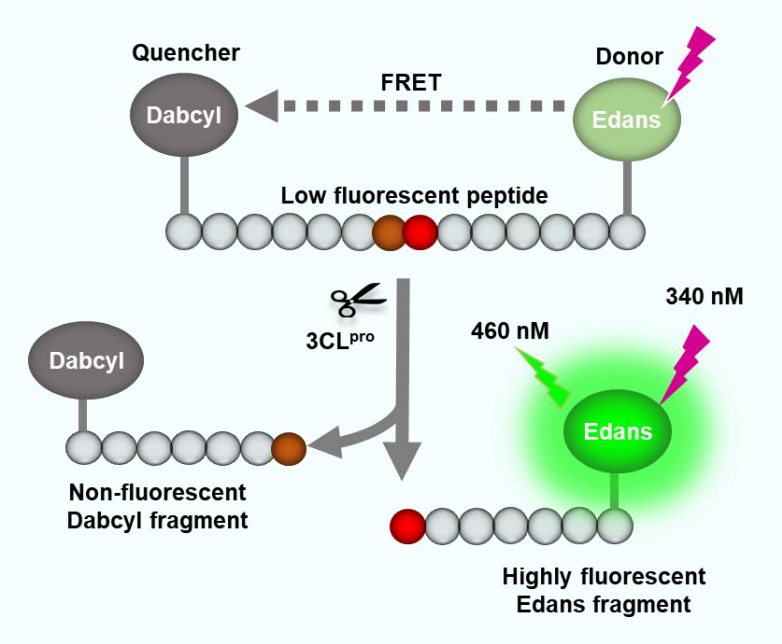

Figure 1. Schematic representation of the fluorogenic SARS-CoV-2 protease enzymatic assay. The peptide substrate exhibits low fluorescent because the fluorescence intensity of Edans in the C-terminal is quenched by the Dabcyl in the N-terminal of the substrate. The protease cleaves the substrate which breaks the proximity of the quencher molecule Dabcyl with the fluorophore Edans, resulting in an increase in fluorescence signal. This increase in fluorescence signal is proportional to the protease activity.

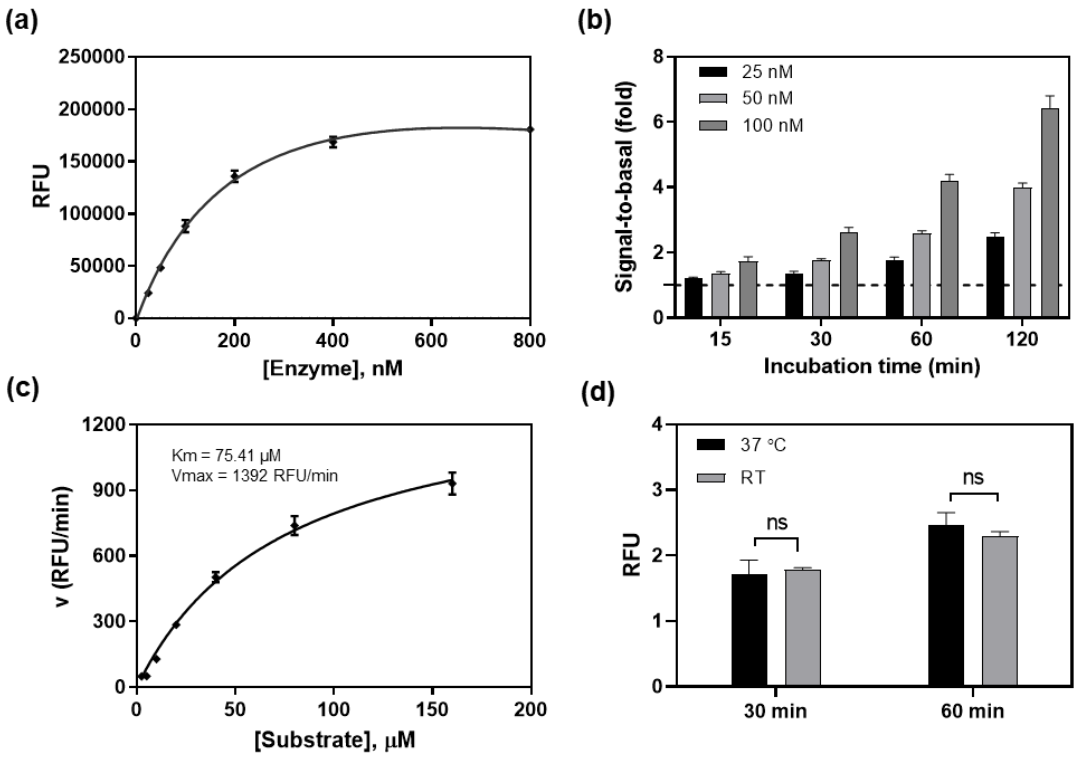

Figure 2. SARS-CoV-2 3CL^{pro} enzyme assay optimization. (a) Concentration-response curve of enzyme titration. With a fixed concertation of substrate (20 μM), the fluorescent intensity increased with enzyme concentrations. The linear response was observed at low enzyme concentrations. Measurement was conducted 2 h after initiating the reaction at RT. (b) The signal-to-basal (S/B) ratios of three enzyme concentrations within the linear range, at various incubation times. Dotted line represents the S/B = 1. (c) Enzyme kinetics. Michealis-Menton plot exhibited a Km of 75.41 μM and Vmax of 1392 RFU/min for SARS-CoV-2 3CL^{pro}. (d) The S/B ratios determined at RT and 37 °C. No difference was observed in 1 h incubation between the two temperatures.

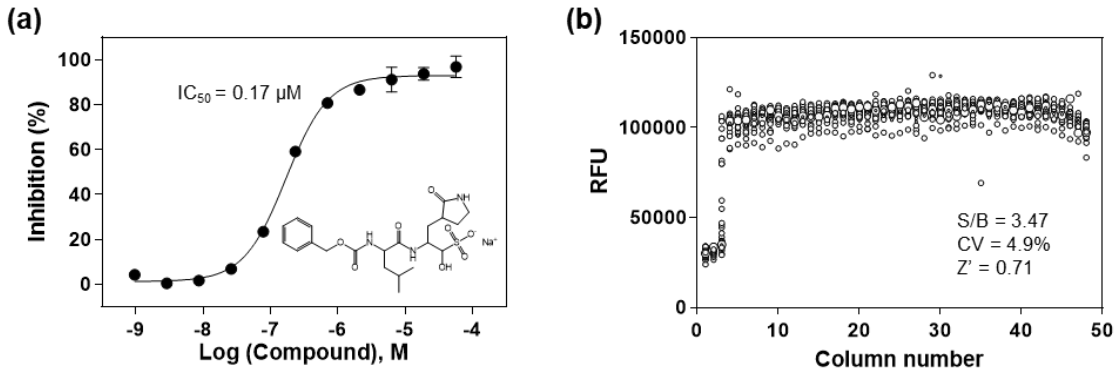

Figure 3. (a) Concentration response of the known 3CL^{pro} inhibitor, GC376. An IC_{50} of 0. 17 μM was determined for the inhibition of SARS-CoV-2 3CL^{pro}. The substrate concentration was 20 μM and enzyme concentration was 50 nM in this experiment. (b) Scatter plot of the results from a DMSO plate in the 3CL^{pro} enzymatic assay in a 1536-well plate, where columns 1 and 2 in the plate contain substrate only, column 3 includes GC376 titration (1:3 dilution series from 57.5 μM), and columns 5-48 contain DMSO (23 nL DMSO in 4 μL reaction solution).

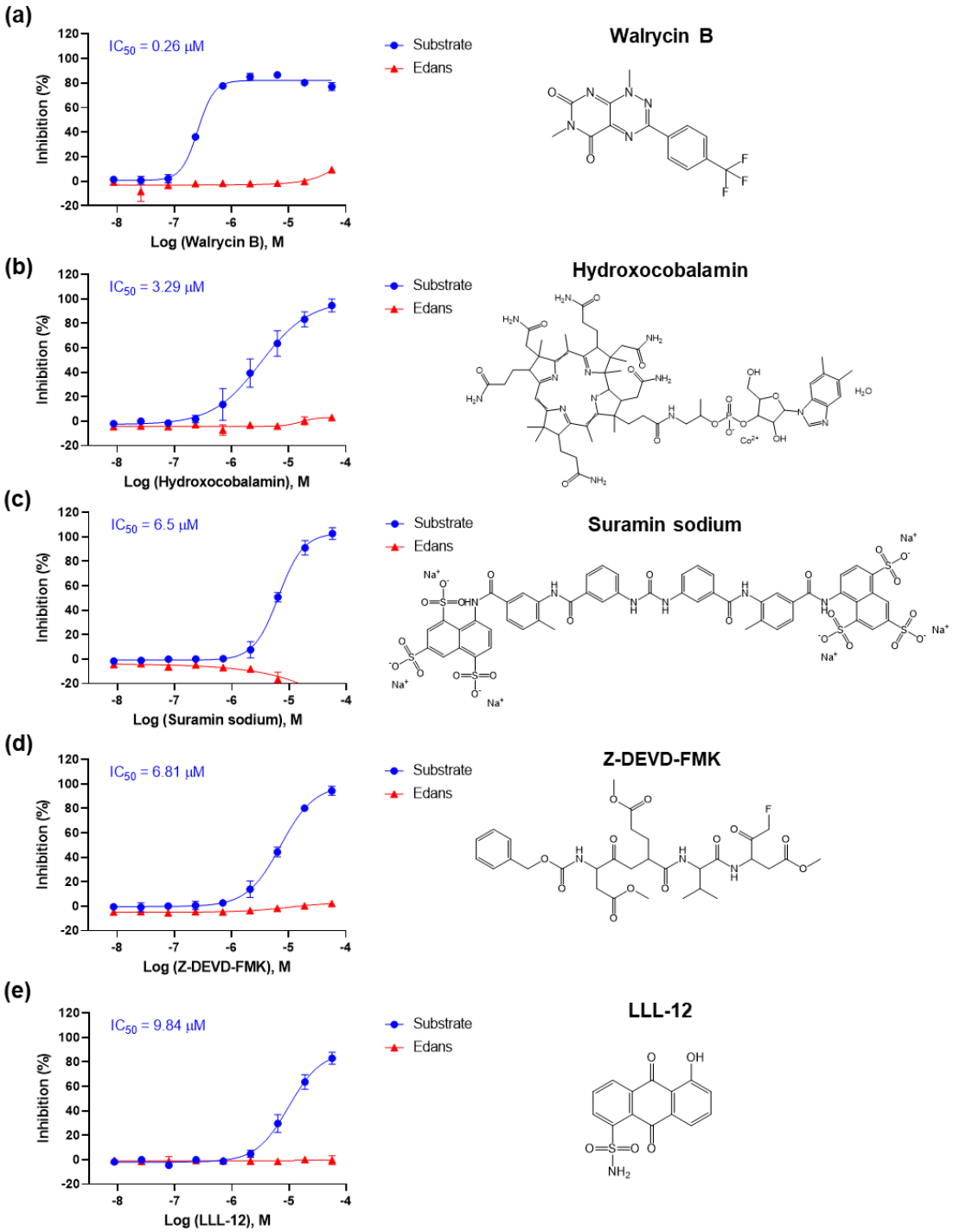

Figure 4. Inhibitory concentration-response curves of the 5 most potent compounds with IC_{50} values < 10 μM and maximal inhibition > 80% determined in the SARS-CoV-2 $3CL^{pro}$ enzyme assay. Red curves show the counter screen results. (a) Walrycin B, IC_{50} = 0.26 μM. (b) Hydroxocobalamin, IC_{50} = 3.29 μM. (c) Suramin sodium, IC_{50} = 6.5 μM. (d) Z-DEVD-FMK, IC_{50} = 6.81 μM. (e) LLL-12, IC_{50} = 9.84 μM.

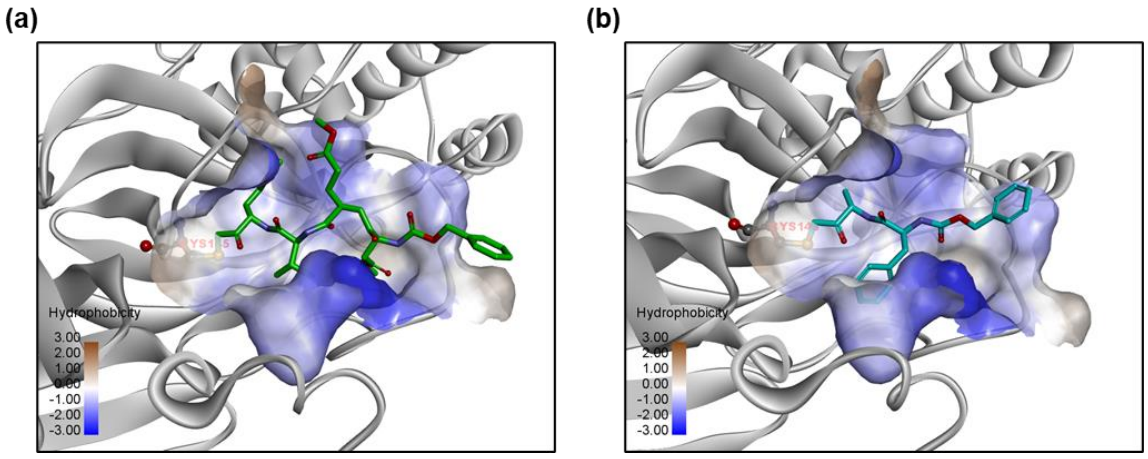

Figure 5. Predicted binding models of (a) Z-DEVD-FMK and (b) Z-FA-FMK bound to the active site of $3CL^{pro}$. The protein $3CL^{pro}$ (grey) is represented in ribbons and the active site is shown with the hydrophobic protein surface. Small molecule inhibitors are shown in sticks. The catalytic residue Cys145 in the binding pocket is highlighted.

SUPPORTING INFORMATION

Additional supporting information may be found online in the Supporting Information section at the end of this article.

Supplementary Information

Identification of SARS-CoV-2 3CL Protease Inhibitors by a Quantitative High-throughput Screening

Wei Zhu[#], Miao Xu[#], Catherine Z. Chen, Hui Guo, Min Shen, Xin Hu, Paul Shinn, Carleen Klumpp-Thomas, Sam Michael, Wei Zheng[*]

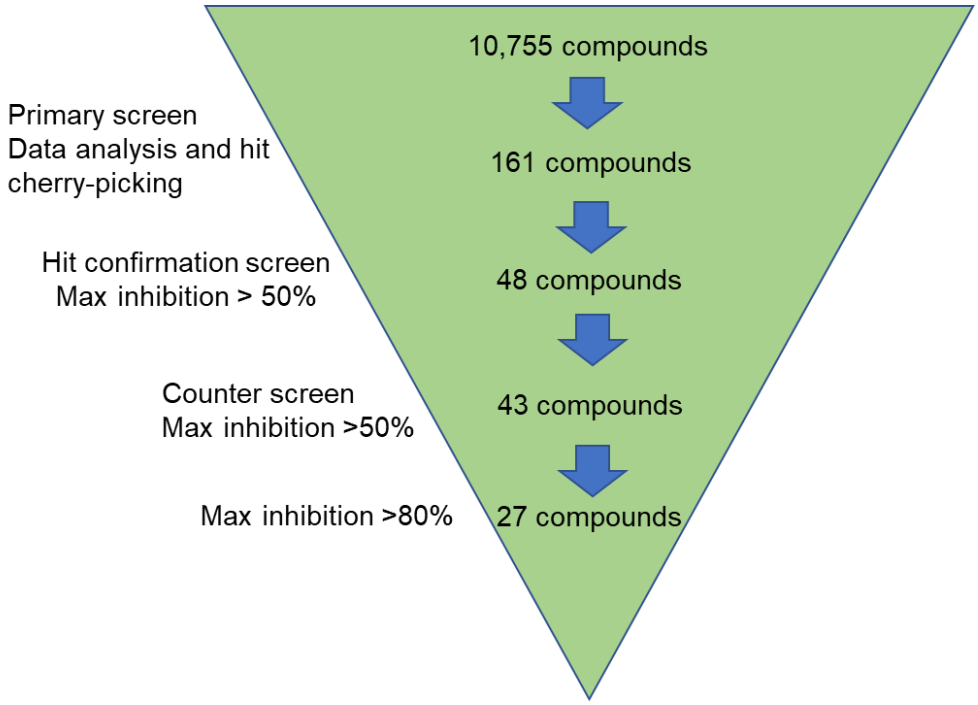

Supplementary Figure 1. Triage strategy used to narrow down the starting 10,755 small molecules from the primary HTS campaign which led to the identification of 27 compounds having IC_{50}s < 30 μM, maximal inhibition > 80% against SARS-CoV-2 $3CL^{pro}$.

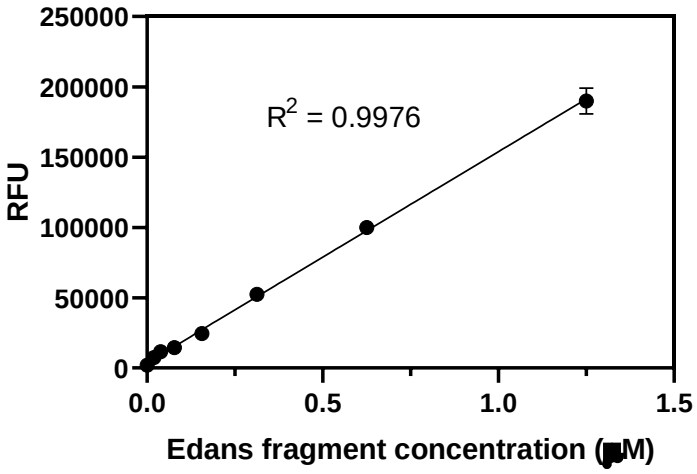

Supplementary Figure 2. Standard curve generated by various dilutions of SGFRKME-Edans (fluorescent fragment in assay byproducts). The relative fluorescent unit (RFU) is linearly proportional to the amount of SGFRKME-Edans.

Supplementary Table 1. Activity of 16 identified compounds with maximal inhibition between 50% to 80% against SARS-CoV-2 $3CL^{pro}$, and their CPE and cytotoxicity.

Compound Name	$3CL^{pro}$ Inhibition		SARS-CoV-2 CPE		Vero E6 Cytotoxicity	
	IC_{50} (μM)	Max Resp (%)	EC_{50} (μM)	Efficacy (%)	CC_{50} (μM)	Efficacy (%)
DA-3003-1	3.04	65.56	3.16	38	1.58	96.02
Fascaplysin	6.81	56.49	N/A, >20	0	1.26	99.28
CAY-10581	8.57	50.59	N/A, >20	0	N/A, >20	0
MG-115	12.1	68.12	0.023	72.005	1	92.35
Sepantronium bromide	12.1	51.47	N/A, >20	0	7.94	20.12
beta-Lapachone	13.58	54.41	N/A, >20	0	12.59	15.06
Vitamin B12	17.1	63.16	N/A, >20	0	N/A, >20	0
4E1RCat	19.18	64.34	N/A, >20	0	N/A, >20	0
THIOSTREPTON	21.52	52.23	N/A, >20	0	N/A, >20	0
TBB	24.15	76.72				
GW-501516	24.15	75.26	5.62	15.5	N/A, >20	0
SP 100030	24.15	63.05	N/A, >20	0	N/A, >20	0
ML193	24.15	56.14	N/A, >20	0	N/A, >20	0
Zafirlukast	24.15	52.98	N/A, >20	0	N/A, >20	0
Sofalcone	24.15	51.64	12.59	60.42	12.59	34.99
TC LPA5 4	27.1	62.28	N/A, >20	0	N/A, >20	0